The *modus operandi* of a DNA enzyme: enhancement of substrate basicity

Yingfu Li and Dipankar Sen

Background: We wished to investigate the mode of catalytic action of a small DNA enzyme (DNAzyme), PS5.M, that, when folded into an appropriate tertiary structure, catalyzes the insertion of copper and zinc ions into porphyrins such as mesoporphyrin IX (MPIX). PS5.M, originally derived from SELEX experiments for specific DNA binders of the distorted porphyrin *N*-methylmesoporphyrin (NMM), had enzymatic parameters ($k_{cat}/K_m = 39{,}700\ M^{-1}min^{-1}$; $k_{cat}/k_{uncat} = 3{,}700$) that rivalled those of an antibody that catalyzed the same reaction.

Results: We used ultraviolet–visible absorption and fluorescence spectroscopy to study the mode of action of PS5.M and related catalytic DNA molecules. We found that the MPIX–DNAzyme complexes had absorption spectra more closely resembling those of the DNAzymes complexed to NMM than to the spectra of MPIX itself, whether MPIX was in its monomeric or aggregated form. pH titration experiments revealed that the DNAzyme raised the protonation pK for MPIX by 3–4 pH units.

Conclusions: Our results reveal that PS5.M works by enhancing the basicity (and hence the ease of metallation) of the bound porphyrin substrate. Large changes in the porphyrin's basicity may be brought about through distortion of the planar porphinato– core of MPIX to resemble that of the naturally deformed porphyrin NMM or through stabilization by a DNA phosphate of the growing positive charge in the transition state for porphyrin protonation/metallation or through a combination of the two. The catalytic strategy of enhancing substrate basicity may also hold true for porphyrin metallation by the recently described catalytic RNA and catalytic antibody for this reaction.

Address: Institute of Molecular Biology and Biochemistry, and Department of Chemistry, Simon Fraser University, Burnaby, British Columbia V5A 1S6, Canada.

Correspondence: Dipankar Sen
E-mail: sen@sfu.ca

Key words: DNAzyme, fluorescence, porphyrin, ribozyme, ultraviolet–visible spectroscopy

Received: **10 October 1997**
Revisions requested: **3 November 1997**
Revisions received: **10 November 1997**
Accepted: **11 November 1997**

Published: **14 January 1998**

Chemistry & Biology 1998, **5**:1–12
http://biomednet.com/elecref/1074552100500001

Introduction

It has been known since the early 1980s [1,2] that certain RNA molecules can catalyze chemical reactions. All of the ribozymes found in nature to date catalyze reactions that break, transfer or form RNA phosphodiesters (reviewed recently in [3,4]), although it has been proposed that RNA catalysis is also responsible for the peptidyl transfer activity of ribosomes [5]. The recent development, however, of powerful technologies for the *in vitro* selection and amplification of catalytic RNA and DNA molecules from large random-sequence libraries ('SELEX'; reviewed in [6–8]) has enabled both the modification of catalytic properties of pre-existing ribozymes, as well as the derivation of artificial ribozymes for the catalysis of novel reactions, ones not characteristic of naturally occurring ribozymes. The rationale for deriving artificial ribozymes that have novel catalytic abilities is to determine the catalytic range of RNA. This knowledge has importance for the 'RNA world' hypothesis [9,10], according to which the RNA molecules capable of catalyzing self-replication as well as the reactions of a simple metabolism might have constituted an early form of life. Interestingly, DNA has also been shown recently to be capable of different kinds of catalysis [11–17]. A comparison of the relative abilities of RNA and DNA to catalyze a given reaction should provide valuable insights into the importance (or lack thereof) of the 2′ ribose hydroxyl functionalities of RNA for the formation of the appropriately folded structures necessary for catalysis, as well as for the catalytic mechanisms themselves.

A class of enzymes in the heme-biosynthetic pathways of different organisms, called ferrochelatases, catalyze the metallation of such porphyrins as protoporphyrin IX (PPIX) and mesoporphyrin IX (MPIX; Figure 1) by Fe^{2+} and other cations. The transition state for this reaction is thought to correspond to distorted forms of the normally planar PPIX and MPIX [18,19], and evidence for this hypothesis has come from the following observations: an *N*-alkyl porphyrin, *N*-methylmesoporphyrin (NMM; Figure 1), has been found to be a strong competitive inhibitor for ferrochelatases [18,20–23]; NMM has a bulky methyl substitution on one of its pyrrole rings and that pyrrole ring is bent out of the plane of the porphyrin. This buckling of the porphyrin has been shown in a number of X-ray crystallographic studies [24–26]. Owing to the resulting ease of access by metal ions to the lone pair electrons of the bent

Figure 1

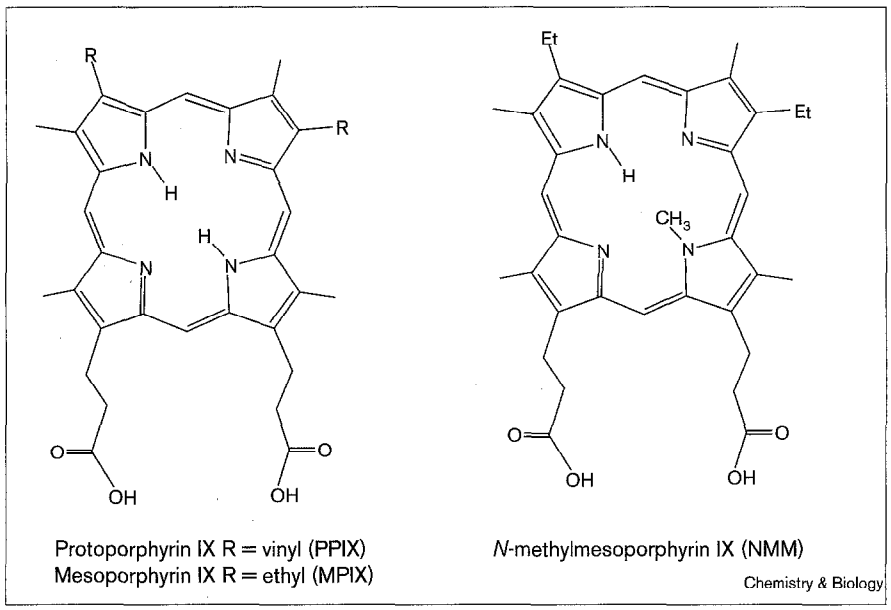

The structures of mesoporphyrin IX (MPIX) and *N*-methylmesoporphyrin IX (NMM).

pyrrole ring, the metallation rate of an *N*-alkyl porphyrin is much higher than that of its non-alkylated counterpart [27–29]. On the basis of its above properties, NMM has been thought to mirror the transition state for the metallation of planar porphyrins such as PPIX and MPIX.

The notion of NMM being a stable transition state analog for the metallation of MPIX was exploited by Cochran and Schultz [19] to generate catalytic antibodies (reviewed in [30]) for porphyrin metallation. Cochran and Schultz obtained monoclonal antibodies that catalyzed the insertion of Zn^{2+}, Co^{2+}, Mn^{2+} and Cu^{2+} into MPIX (although not into PPIX or other, related, porphyrins). Subsequently, two groups used NMM and SELEX strategies to derive nucleic acid molecules that also catalyzed this reaction: Schultz and coworkers [31] reported a catalytic RNA, while Li and Sen [14] reported a catalytic DNA.

The optimal conditions for the functioning of DNAzymes for porphyrin metallation have been examined in some depth and have been reported [14,32]. The DNA molecule that was both the optimal and the minimal sequence for this catalysis (named PS5.M) was only 24 nucleotides long (see the Materials and methods section for DNA sequences). Its catalytic activity, inserting Cu^{2+} or Zn^{2+} ions into MPIX or PPIX, required potassium ions for the proper folding of the oligomer. The very guanine-rich oligomer probably formed a guanine quadruplex (reviewed in [33,34]) for its catalytically active structure. The optimal pH for catalysis was found to be 6.2 and the optimal temperature was ~40°C. Following a series of optimization steps taken to enhance its activity, PS5.M was found to be a good catalyst with enzymatic parameters (k_{cat}/K_m = 39,700 M^{-1} min^{-1}; k_{cat}/k_{uncat} = 3,700 for copper insertion into PPIX, measured at a fixed copper concentration of 1mM) that compared well with those of the above-mentioned catalytic RNA and catalytic antibody.

The optimization steps, however, did not provide any information about the mode of catalytic action by PS5.M. Although the original selection strategy for the derivation of PS5.M [14,35] had sought DNA molecules that bound preferentially to NMM (as compared to MPIX) with the expectation that such molecules might then catalyze porphyrin metallation by distorting bound MPIX to resemble NMM, it was not strictly possible to rule out the possibility that PS5.M might catalyze metallation via some other mechanism. Evidence of this kind has also been lacking for the catalytic RNA and antibody for porphyrin metallation mentioned above [19,31]. In this paper, we provide direct spectroscopic evidence that PS5.M and its related DNA sequences work by enhancing the basicity of bound substrate porphyrins.

Results and discussion

The effect of nonionic detergents on the solubility and ultraviolet–visible absorption properties of MPIX and NMM

MPIX

MPIX is a very hydrophobic molecule and has very low solubility in water or in buffered solutions around neutral pH. As a consequence of its hydrophobic character, MPIX, as well as a number of its metallo-derivatives, tends to aggregate by forming dimers or polymers in a time-dependent manner in aqueous solutions [36–41]. For instance, MPIX starts to form dimers at concentrations as low as

0.05 μM [40]. Experimentally, this problem is, however, usually overcome by the inclusion of detergents in the assay buffers [42,43]. Such detergents may be anionic (e.g., sodium dodecyl sulfate; SDS), cationic (e.g., cetyltrimethyl ammonium salts) or nonionic (e.g., detergents of the Tween and Triton series). Nonionic detergents such as Triton X-100 and Tween 20 have been widely used in ferrochelatase enzyme assays to solubilize and render monomeric the hydrophobic porphyrin substrates [42–45]; our own earlier work on the DNAzymes PS5.ST1 and PS5.M was also carried out in buffers containing 0.1–0.25% Triton X-100 [14,32].

We investigated the effect of the nonionic detergent Triton X-100 on the absorption properties of MPIX. The solubility of MPIX in 40K buffer (buffer lacking any detergent — see the Materials and methods section) was extremely low. For 2 μM MPIX in 40K buffer, no absorption could be detected even in the strongly absorbing Soret region ($\varepsilon \simeq 2.5 \times 10^5\ cm^{-1}\ M^{-1}$, in 40K + T buffer; see the Materials and methods section) after the solution had been centrifuged at 13,000 r.p.m for 30 min. The solubility of MPIX increased with increasing Triton concentration (reflected, among other things, in the fact that higher and higher absorption intensities could be measured in the supernatants following the 30 min spin treatments of MPIX–Triton solutions). Figure 2 shows that the absorption intensities of uncentrifuged MPIX– Triton solutions increased with progressively higher Triton concentrations in both the Sorct region (~400 nm) and the visible region (peaks I, II, III and IV between 500–700 nm; numbered according to Smith [43]). The absorption intensities reached saturation at a Triton concentration of 0.085%. Correspondingly, at this Triton concentration, no MPIX precipitation could be detected by centrifugation (data not shown). The solubility and absorption properties of MPIX were also tested in the presence of other nonionic detergents, namely, Tween 20, and Nonidet P-40. Both had effects essentially indistinguishable from that of Triton X-100 (data not shown).

NMM

Unlike MPIX, *N*-methylmesoporphyrin IX (NMM) was both more soluble and less prone to aggregation in water and in buffered neutral solutions. For instance, no precipitation was detected in 1–5 μM NMM solutions in the detergent-free buffer, 40K. Nonionic detergents such as Triton X-100 and Tween 20, tested up to 0.1% (w/v), did not show a significant effect on either the solubility or the absorption of NMM within this concentration range. The higher solubility of NMM in the neutral aqueous solutions was most probably due to the higher basicity of NMM than MPIX [18,43]. At neutral pH, NMM exists mainly in a mono-protonated form, with a positively charged center, whereas MPIX is not substantially protonated [18,43].

Figure 2

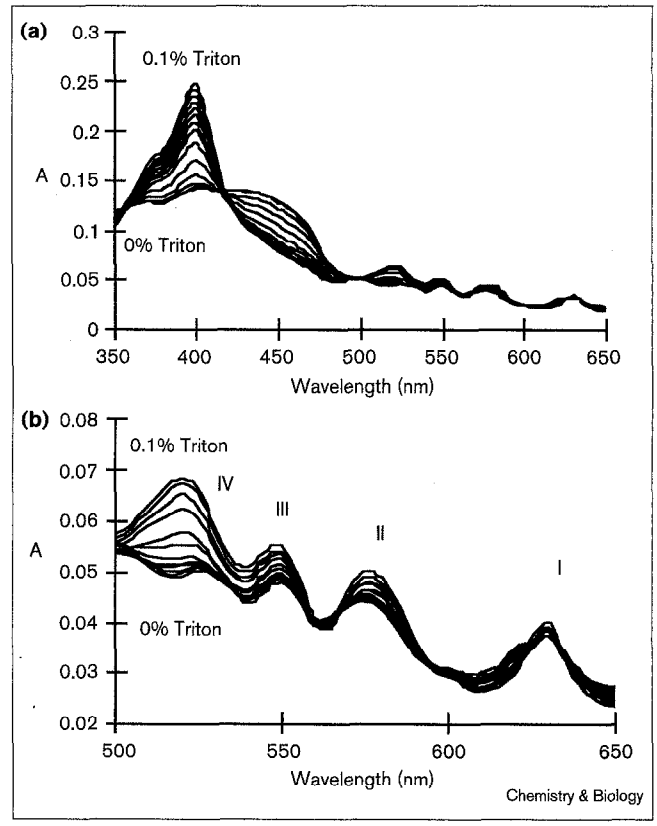

Absorption spectra of MPIX with increasing detergent concentrations. **(a)** Absorption from 350 to 650 nm; **(b)** absorption from 500 to 650 nm. MPIX (2 μM) was titrated in 40K buffer with the following Triton concentrations: 0, 0.005, 0.0075, 0.01, 0.0125, 0.015, 0.0175, 0.02, 0.025, 0.03, 0.035, 0.06, 0.085 and 0.1%.

The effects of PS5.ST1 and other DNA oligomers on the solubility and absorption properties of MPIX and NMM

We wished to investigate whether binding to DNAzymes such as PS5.ST1 (a 33 nucleotide sequence precursor of PS5.M) affected the ultraviolet (UV)–visible spectra of MPIX. Spectral measurements were therefore made at a fixed concentration of MPIX (1 μM, in 40K buffer) titrated with progressively higher concentrations of PS5.ST1, ranging from 0 to 366 μM. In the absence of DNA, or at the lower DNA concentrations, the MPIX spectrum resembled that of the aggregated form of the porphyrin (see Figure 2). At the higher DNA concentrations, however, the initially broad Soret band sharpened (as in the presence of Triton) to a well-defined peak, centered at 399 nm, the intensity of which increased with PS5.ST1 concentrations until a saturation of intensity occurred around 100 μM PS5.ST1. Figure 3a shows that this DNA-enhanced Soret peak generally resembled in shape and intensity the Soret peak seen in the presence of Triton; a slight distinguishing feature between the two was that in Triton a small shoulder appeared (at 375 nm) on the body of the Soret peak, whereas in the PS5.ST1 samples this was not present.

Figure 3

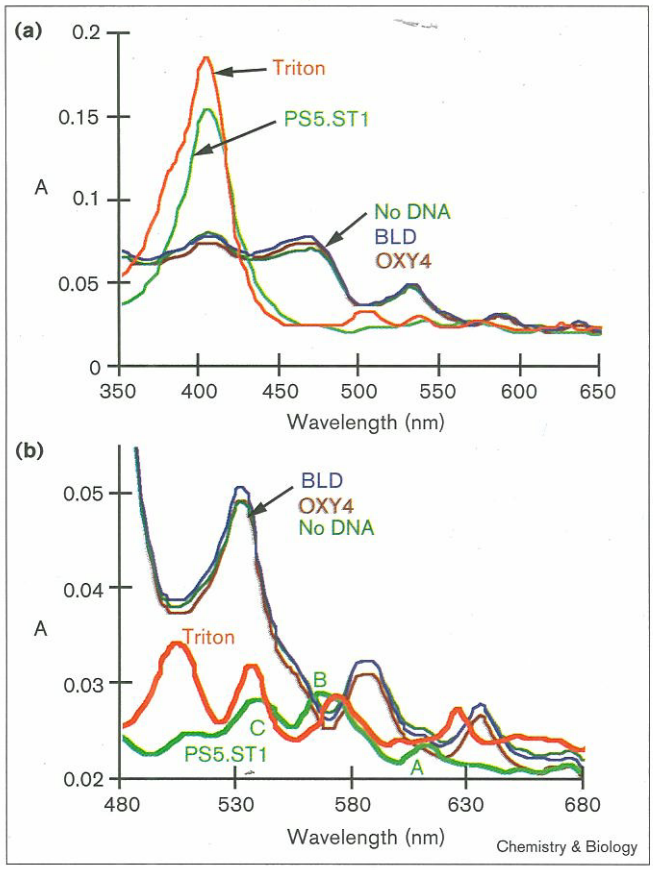

Absorption spectra of MPIX in the presence of different DNA oligomers. MPIX was at 1 μM, and the DNA concentrations were 10 μM. **(a)** MPIX spectra (in 40K buffer) from 350 nm to 650 nm, in the absence of DNA oligomers but in the presence of 0.1% Triton; in the presence of the control oligomers BLD or OXY4; and in the presence of the catalytic sequence PS5.ST1. **(b)** The spectral region from 480 nm to 680 nm.

In the visible (480–680 nm) region (Figure 3b), the pattern of absorption maxima and the location of these maxima were utterly distinctive following titration with the DNAzyme. The MPIX–PS5.ST1 complex showed a completely different absorption peak profile (an A–B–C pattern) from that found in the presence of Triton or other detergents. MPIX–Triton had major absorptions peaking at ~510 nm (peak IV), ~540 nm (peak III), ~570 nm (peak II), and ~630 nm (peak I). The intensity of these peaks decreased in the order of: IV > III > II > I (Figure 2). The new A–B–C peak pattern had maxima at ~540 nm, ~565 nm and ~610 nm, respectively, with intensities in the order of B > C > A.

To determine whether the MPIX spectral changes seen in the presence of PS5.ST1 were mirrored in the presence of other catalytic DNA oligomers, and also to investigate whether the changes could be observed in the presence of any DNA oligomer, spectral titrations of 1 μM MPIX were carried out with progressively increasing concentrations of several different DNA oligomers. In the presence of 10 μM of the catalytic oligomer PS5.M, the spectrum was essentially identical to that found with PS5.ST1. Figure 3 shows the absorption spectra (in 40K buffer) of MPIX in the absence of DNA, in the presence of 10 μM BLD (a noncatalytic control DNA), and in the presence of 10 μM OXY4 (a noncatalytic but G-quadruplex-forming DNA sequence [32]). BLD and OXY4 had no effect on the 'aggregated' absorption of MPIX. To demonstrate that MPIX bound to and was solubilized by PS5.M and PS5.ST1, but not by the other two DNA oligomers, we recorded the absorption spectra of all the above samples following 30 min centrifugations at 13,000 r.p.m. Solutions containing either no DNA or containing the non-catalytic oligomers BLD or OXY4 showed essentially no residual absorption in the supernatant following the spin. By contrast, approximately 70% of the pre-spin absorption intensity persisted in the supernatant of the DNAzyme-containing samples. Similar enhancements of both MPIX solubility and absorption were observed also in the presence of three other catalytic sequences, PS19.ST1, PS2.M and TM.M2 (data not shown).

The effect of Triton on the spectrum of a preformed MPIX–PS5.ST1 complex

The above DNA–MPIX interaction experiments were carried out in 40K buffer. The spectral effect of adding detergent to a preformed DNAzyme–MPIX complex was now examined. A preformed PS5.ST1–MPIX complex (consisting of 1 μM MPIX and 10 μM DNA) was titrated with increasing concentrations of Triton X-100, up to 0.02%. Figure 4 shows that the introduction of Triton into the PS5.ST1–MPIX sample resulted in the absorption spectrum changing to a pattern characteristic of Triton–MPIX spectra: for instance, the shoulder seen at the blue edge of the Soret peak appeared (Figure 4a), and a I–II–III–IV peak pattern (rather than an A–B–C pattern) was now seen in the visible region (Figure 4b). These results indicated that Triton X-100 was able to compete favorably with PS5.ST1 for MPIX binding. This result was consistent with our earlier data that Triton had a negative effect on the catalyzed rate of metallation by PS5.M [32]. The high hydrophobicity of MPIX was probably the most relevant factor for the net movement of MPIX out of the DNAzyme's active site (possibly a site of reasonable hydrophobicity) into Triton micelles with highly hydrophobic interiors.

The NMM–PS5.ST1 complex

The DNA molecules catalytic for porphyrin metallation discussed in this paper were originally selected for their preferential binding of NMM (and poorer binding of MPIX). To study DNAzyme interactions with NMM, we recorded, separately, the UV–visible spectra of NMM dissolved in 40K buffer (lacking detergent), in 40K buffer but with increasing concentrations of Triton, and in 40K buffer in the presence of increasing concentrations of PS5.ST1.

Figure 4

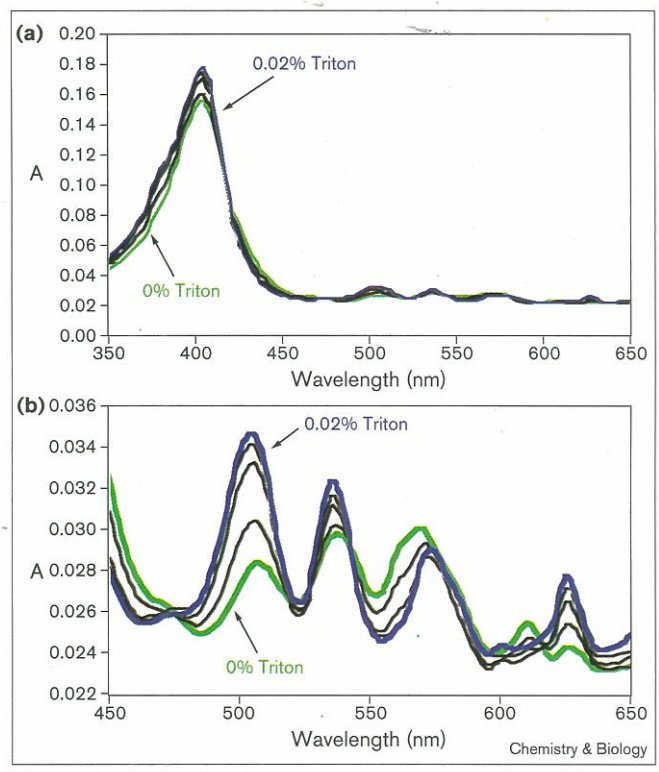

The effect of Triton on the absorption spectra of the MPIX–PS5.ST1 complex. **(a)** The absorption spectra from 350 to 650 nm of preformed PS5.ST1–MPIX, titrated with different Triton concentrations. PS5.ST1 was at 10 μM, MPIX at 1 μM, and Triton was added to 0, 0.005, 0.01, 0.015 and 0.020% concentrations, respectively. **(b)** The region of the spectra from 450–650 nm.

In contrast to the case of MPIX, the presence of increasing concentrations of Triton (tested up to 0.1% Triton X-100) did not significantly change the NMM spectrum (data not shown). This was, undoubtedly, related to the greater hydrophilic character (and a lesser tendency to aggregation) of NMM [46]. The presence of increasing concentrations of PS5.ST1 also had a relatively small effect on the NMM absorption in both the Soret and visible regions. The Soret peak, in the presence of PS5.ST1, shifted approximately 5 nm to the red, with an accompanying small hypochromicity. In the visible region, the presence of PS5.ST1 induced a degree of hyperchromicity in the 570 nm and 615 nm absorbances, but did not grossly change the pattern or the positions of the absorption maxima. Overall, these observations with NMM offered a marked contrast to the various (and significant) spectral changes induced in the MPIX absorption by Triton and by PS5.ST1.

In another striking departure from the case of MPIX, preformed NMM–PS5.ST1 complexes did not dissociate in the presence of concentrations of added Triton (up to 0.1%, data not shown). Undoubtedly, this was again a reflection of a significantly higher binding affinity of the DNAzyme for NMM (compared with MPIX). To determine the affinities of the DNAzyme for the two porphyrins, we initially obtained absorption spectra from separate titrations of MPIX and NMM with catalytic DNA sequences to obtain dissociation constants (K_d). The absorbances, A, for both NMM and MPIX (in the presence of defined concentrations of DNA) were plotted as functions of the DNAzyme concentration. For NMM titrated with the catalytic DNA sequences PS5.M and TM.M2, A versus DNA concentration gave plots characteristic of very tight binding modes [47], whereas MPIX gave evidence of much weaker binding. Figure 5a shows the data for the MPIX titrations. Using a formalism described by Wang *et al.* [48], a K_d value of 6.9 μM ± 0.2 μM was calculated for the MPIX–PS5.M complex. In the case of NMM, to obtain interpretable data, absorbance could not be used. We therefore measured the K_d for the NMM–PS5.M complex using fluorescence (F), with a very low concentration of NMM (25 nM, the lowest possible concentration of NMM consistent with accurate fluorescence measurements) and DNA concentrations between 0 and 600 nM. Figure 5b shows these data: the NMM–PS5.M complex had a K_d value ≤ 7.2 nM ± 0.2 nM. Cumulatively, these data indicated that under solution conditions favoring both optimal binding and optimal catalysis (i.e., 40K buffer [32]) the NMM-binding affinity of PS5.M was ~1000-fold stronger than its affinity for MPIX.

DNAzyme-bound MPIX has an absorption spectrum closely resembling those of NMM and the NMM–DNAzyme complex

In comparing the various absorption spectra described above, a most interesting observation was made. Figure 6 shows a superimposition of the spectra of the monomeric MPIX (in Triton solution), the MPIX–PS5.ST1 complex, and the NMM–PS5.ST1 complex. The spectrum of the MPIX–PS5.ST1 complex, while very different from that of either MPIX alone (i.e., in the aggregated form) or the MPIX–Triton solution, closely resembled the spectrum of the NMM–PS5.ST1 complex across the Soret and visible regions. In the Soret region (Figure 6a), the spectra of the two complexes differed in intensity but were indistinguishable in every other respect — the Soret peaks, with overlapping maxima, were both symmetric peaks with no observable shoulders. In the visible region (Figure 6b), the affinities were even more striking, with the MPIX–PS5.ST1 complex showing an A–B–C peak pattern (like the NMM–PS5.ST1 complex) rather than the I–II–III–IV pattern of MPIX–Triton.

The difference in the visible spectra of NMM (the A–B–C pattern, see above) and of MPIX (the I–II–III–IV pattern, also above) is fundamentally related to their protonation states at neutral pH [43], in that NMM is substantially mono-protonated at this pH, whereas MPIX is not protonated [43]. Generically, neutral porphyrins are both very weak acids (both pKa_1 and pKa_2 for etioporphyrin, in the

Figure 5

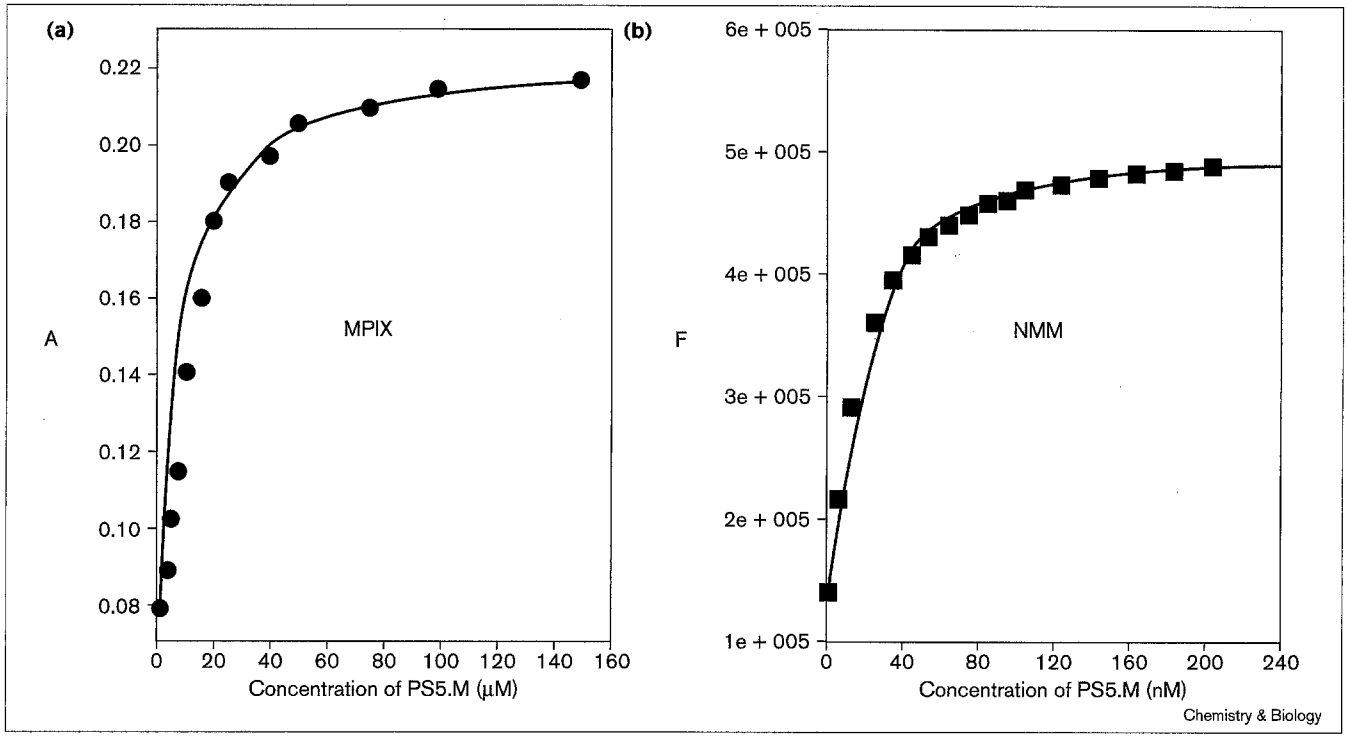

Binding curves of MPIX (via absorbance data) and of NMM (via fluorescence data) to the DNAzyme, PS5.M. **(a)** Absorbance of MPIX (1 μM) when titrated by 0–150 μM PS5.M, in 40K buffer. Absorbance was measured at 399 nm. **(b)** The fluorescence intensity of NMM (25 nM) when titrated by 0–200 nM PS5.M, in 40K buffer. Excitation was at 397 nm. Emission was measured at 610 nm. The measured K_d values were 6.9 ± 0.2 μM (MPIX) and 7.2 ± 0.2 nM (NMM).

scheme shown below, have been estimated at ~16 [43]). Porphyrins are also weak bases. A free-base porphyrin (PH_2) may therefore accept two protons to its imine-type nitrogen atoms to form monocations (PH_3^+) and dications (PH_4^{2+}), as shown below:

$$PH_4^{2+} \overset{pKa_4}{\rightleftharpoons} PH_3^+ \overset{pKa_3}{\rightleftharpoons} PH_2 \overset{pKa_2}{\rightleftharpoons} PH^- \overset{pKa_1}{\rightleftharpoons} P^{2-}$$

The metallation process (i.e., the coordination of the positively charged metal ion to the neutral porphyrin), in the uncatalyzed reaction, is related to the second step (the first protonation event of the neutral porphyrin, with pKa_3) in the scheme above (reviewed in [18]). The uncatalyzed rate-determining step does not involve the PH^- or the P^{2-} species (which have very high pK values, around +16) [43], nor does it involve the loss of liganded waters from such ions as copper (II) and zinc or the formation of outer sphere complexes between porphyrin and metal [18]. Also, in a prior study, we had shown that the PS5.M-catalyzed metallation reaction had a very similar pH profile to that of the uncatalyzed reaction (both rates peaking at pH ~6.2) [32]. We can therefore deduce with some confidence that the DNAzyme-catalyzed reaction and the uncatalyzed reaction share the same rate-determining step. We can now define a quantity 'pKm', or 'metallation pK', as being equivalent to the quantity pKa_3 above. A number of investigators have studied the absorption spectra of the different protonated forms of porphyrins, and found that many porphyrins have generalized and predictable absorption peak patterns for their neutral (PH_2), monoprotonated (PH_3^+) and diprotonated (PH_4^{2+}) forms [43,49–52]. Fundamentally, the visible absorption of the PH_2 form has a I–II–III–IV (four peaks) pattern, the PH_3^+ form has an A–B–C (three peaks) pattern, whereas the PH_4^{2+} species has an X–Y (two peaks) pattern. The existence of these distinct patterns of peaks for the different protonated forms of porphyrins facilitates the measurement of the various pKa values via pH titration experiments.

With regard to substantially planar porphyrins such as MPIX, an interesting observation has been made that in aqueous solution (containing nonionic detergents), only the neutral (PH_2) and the diprotonated species (PH_4^{2+}) are readily observed [43,49,53]. Thus, only a single, and surprisingly low, pKa value of ~2 ($pKa_3 + pKa_4$) was measured for the dimethyl ester of MPIX [43,49,53]. The failure to observe the mono-protonated species has been attributed to the difficulty of protonating the sterically crowded cavity (with two hydrogens present already) of structurally flat porphyrins such as MPIX. The initial protonation

Figure 6

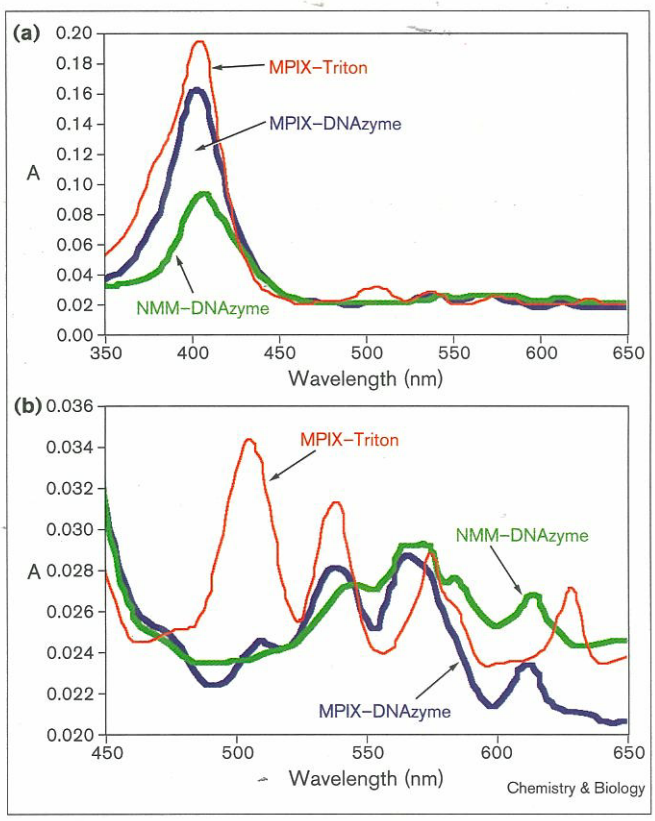

Similarities between the absorption spectra of the DNAzyme–MPIX and DNAzyme–NMM complexes. **(a)** The spectra from 350 to 650 nm and **(b)** the visible region of the spectra.

Figure 7

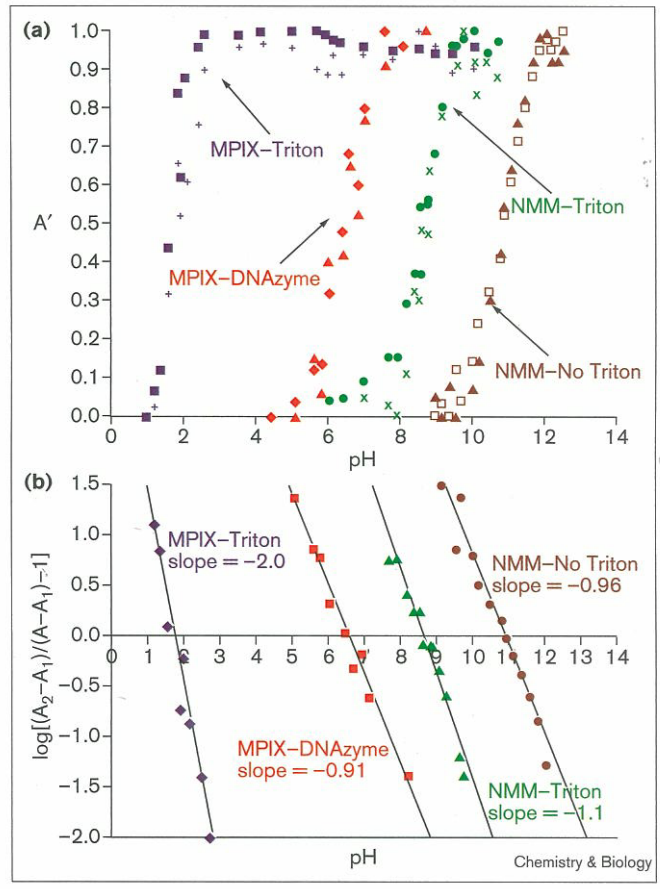

(a) Normalized pH titration curves for MPIX–Triton, MPIX–PS5.M, NMM–Triton and NMM in the absence of both Triton and PS5.M. A′: all absorbances were normalized, with a value of 1.0 at the higher pH end and 0 at the lower pH end. MPIX was at 1 μM, NMM at 3 μM, Triton X-100 at 0.1% and PS5.M at 20 μM (where applicable). MPIX–Triton (blue; + at 500 nm, and ■ at 397 nm); MPIX–DNAzyme (red; ◆ at 500 nm and ▲ at 604 nm); NMM–Triton (green; ● at 397 nm, and × at 568 nm); NMM–no Triton (brown; □ at 397 nm, and ▲ at 560 nm). **(b)** Plots of log $[(A_2 - A_1)/(A - A_1) - 1]$ versus pH for samples shown in (a). The MPIX–Triton points were from the 397 nm data (see above), the MPIX–DNAzyme from the 500 nm data; NMM–Triton from 397 nm, and NMM–no Triton from 397 nm. Data from measurements made at the other wavelengths for each sample gave straight lines in excellent agreement with those shown.

event (to give PH_3^+), however, is thought to distort the porphyrin away from the planar and to facilitate a rapid second protonation [52,53]. Crystal structures of mono- and diprotonated porphyrins have, in fact, shown that these porphyrins do have bent structures, with one pyrrole unit being tilted ~15° away from the plane of the mono-protonated species and ~30° of the plane of the diprotonated species [53,54]. In concordance with this notion, naturally non-planar porphyrins (such as the *N*-alkyl porphyrins, including NMM) undergo protonation with a significantly greater facility than do planar porphyrins (such as MPIX). Owing to their distorted structures, the basicity of *N*-alkyl porphyrins is significantly greater, and the pKa values for their first protonation are typically 3–5 pH units higher than those of corresponding non-alkylated, planar porphyrins. The pKa values for the second protonation, however, are not significantly different between the two groups, as expected [18,46].

The effect of DNAzyme-binding on the pKm values of NMM and MPIX

We carried out pH titration experiments to determine the pKm values of NMM and of MPIX under our experimental conditions, in both the presence and absence of saturating concentrations of the DNAzyme PS5.M. Absorbance changes, monitored at different wavelengths (see legend for Figure 7) were measured as functions of pH for NMM alone (in water and in 0.1% Triton solution), for MPIX alone (in 0.1% Triton solution), as well as for the two porphyrins bound to PS5.M. The absorbance changes (normalized to a scale of 0–1.0) are shown in Figure 7a. The pKm values (the midpoint pH values for the various sigmoidal curves) can be accurately determined by plotting the quantity log $[(A_2 - A_1)/(A - A_1) - 1]$ as a function of pH. These plots are shown in Figure 7b (the pKm of NMM bound to

Table 1

pKm values for MPIX and NMM in various solutions.

Porphyrin	In 0.1% Triton	No detergent	PS5.M
MPIX			
(UV–visible)	1.8*	N/A	6.6
(fluorescent)	1.8*	2.8	6.4
NMM			
(UV–visible)	8.7	10.8	> 10

*Value for pKa_3 and pKa_4.

PS5.M could not be obtained since the folded structure of the DNAzyme could not be preserved above pH 10) and the pKm values obtained (the x intercepts in Figure 7b) are listed in Table 1. The PS5.M–MPIX complex had a pKm of 6.5, which was vastly higher than that of MPIX in Triton solution (1.8), but closer to that of NMM, whether in Triton solution (8.6) or in water (10.8). This unexpected result indicated that a measurable consequence of interaction with the DNAzyme was a strong enhancement of the basicity of MPIX to a value closer to the basicity of the distorted porphyrin NMM.

It is interesting to note also from Figure 7b that the negative of the slope for log $[(A_2–A_1)/(A–A_1) – 1]$ as a function of pH (see Calculations in the Materials and methods section) was ~2 for the MPIX samples in Triton solution, whereas the others gave values of approximately ~1. The slope of ~2 was fully consistent with that protonation event having two protons added to the neutral MPIX, as discussed above. MPIX bound to DNAzyme, however, acquired a single proton.

Prior to attempting an analysis of the data presented above, it was necessary to investigate the possible perturbation of porphyrin pKm values by the detergent (0.1% Triton) present in the buffers used for the measurements on MPIX in the absence of added DNAzyme (this was the only absorbance sample which, owing to the poor solubility of MPIX, required detergent). A direct absorbance measurement of the pKm of MPIX dissolved in water without detergent could not be made, owing to the poor solubility and tendency of MPIX to aggregate in detergent-free buffers. We therefore made pH titrations using fluorescence, at very low (10 nM) MPIX concentrations, to directly determine the pKm of detergent-free MPIX. Figure 8a–c shows the fluorescence spectra across broad pH ranges of MPIX in a 0.1% Triton solution (Figure 8a), MPIX in a water solution without any Triton (Figure 8b), and MPIX in the presence of 1 μM PS5.M (a 100-fold molar excess over the porphyrin, to assure full binding of the porphyrin — Figure 8c). That the detergent-free solution of MPIX at this low porphyrin concentration was indeed a true solution was confirmed first by the persistence of fluorescence

Figure 8

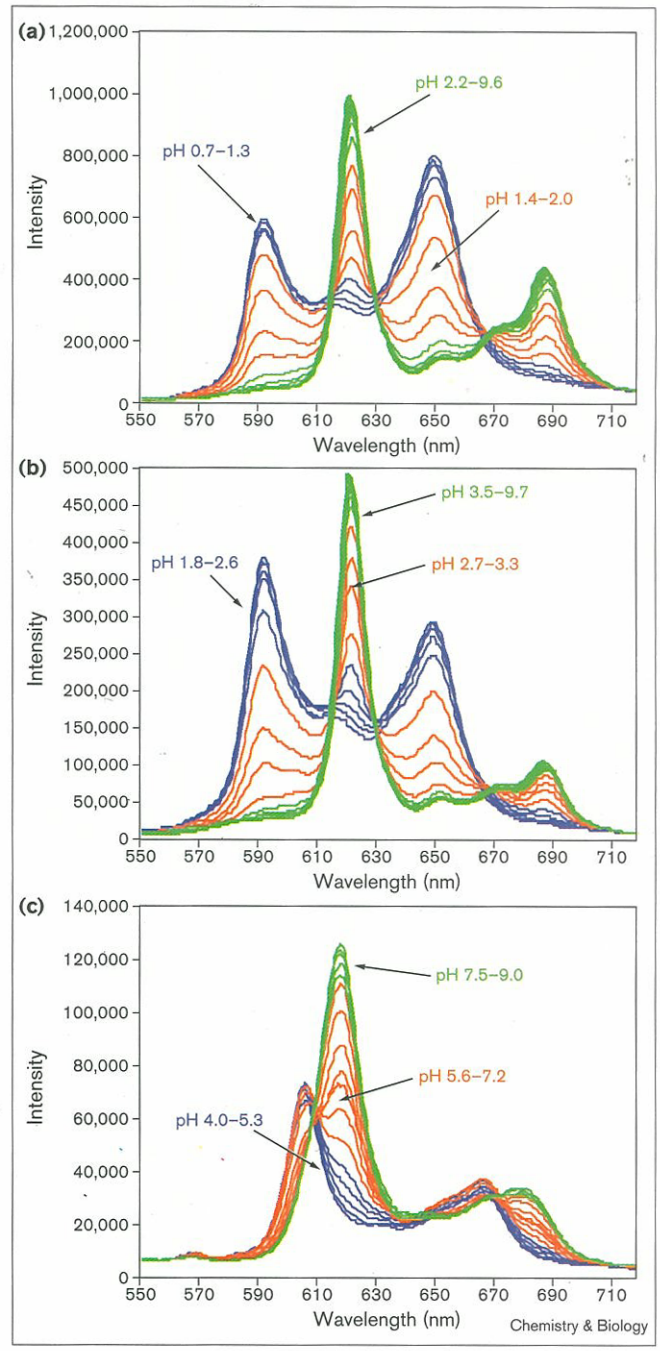

Fluorescence emission spectra as functions of pH. **(a)** MPIX in a 0.1% Triton solution; **(b)** MPIX in solution without Triton; **(c)** MPIX complexed to the DNAzyme PS5.M. MPIX concentrations in all samples were 10 nM; PS5.M concentration in (c) was 1 μM. The excitation wavelength in each case was 397 nm.

intensities in this sample following the high-speed spin for 30 min (which, as described above, successfully pelleted undissolved porphyrin), and second by the essential similarity of the spectra in the absence as well as in the presence of Triton. It is interesting to note, in this context, that the

DNAzyme–MPIX complex had a qualitatively differently spectrum from the other two MPIX spectra, especially in the low pH regime. Undoubtedly, this reflected our earlier finding (above) that MPIX by itself underwent a double protonation event, with a single pK value, whereas MPIX bound to the DNAzyme acquired only a single proton.

Our above conjecture could be checked, as well the individual pKm values we desired obtained, from a plot of log $[(F_2 - F_1)/(F - F_1) - 1]$ as a function of pH. Figure 9 shows that the plots of MPIX (in water solution and in Triton solution) had slopes of ~2, indicating double protonation events whereas the slope of the DNAzyme–MPIX complex had a slope of ~1. Second, it can be seen that the 'true' pKm of MPIX, in the absence of Triton, was 2.8 (approximately one pH unit higher than in the presence of the detergent). The pKm change caused by the DNAzyme binding to MPIX was 6.5 – 2.8 = 3.7 pH units. In other words, the DNAzyme appeared to contribute to an enhancement of the basicity of MPIX by between three and four pH units.

Figure 9

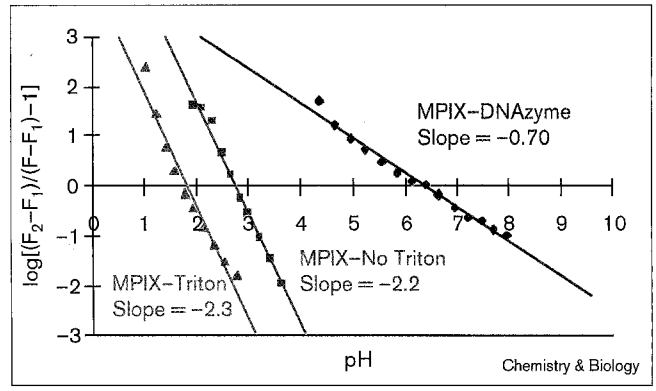

Plots of log $[(F_2 - F_1)/(F - F_1) - 1]$ versus pH for samples shown in Figure 8.

How does the DNAzyme enhance MPIX basicity by ~3.7 pH units?

How might the DNAzyme influence the basicity of bound porphyrins? There are three possible means: first, by providing a binding environment for the porphyrin with a dielectric constant different from that of the surrounding water; second, by positioning a negative charge close to the porphyrin binding site in order to stabilize the positive charge developing in the porphyrin core as it is being protonated or metallated; and third, by distortion of the planar porphyrin to make more accessible to protons (or to metal ions) one or more set of pyrrole nitrogen lone pairs. It is likely that the DNAzyme's binding site does supply a significantly hydrophobic environment to the bound porphyrin; however, such an environment would, if anything, make a porphyrin less basic, as the charge of the monoprotonated porphyrin would find poorer solvation in such an active site than in the bulk water. If the first possibility might thus be eliminated, how might it be possible to distinguish between the other two?

Micelles formed from an anionic detergent such as SDS provide a potentially interesting model system for the above problem, for they should in principle be capable of supplying to MPIX molecules bound to them both a hydrophobic environment as well as proximal negative charges. SDS, when packed into a regular and tightly packed structure such as a micelle, should display the characteristics of a polyanion, with each SDS molecule contributing one full negative charge per 250 Da molecular weight (whereas DNA contributes one full negative charge per 300–330 Da). Additionally, one might expect that binding to such micelles would not distort the planarity of the porphyrin. SDS micelles therefore might provide a simple model system for testing the relative effects of porphyrin structural distortion (the third possibility, above) and of active-site environmental effects (the second possibility) on the basicity of bound porphyrins. pKm measurements were therefore made of 1 μM MPIX fully dissolved in a solution of 1% SDS (35 mM SDS, significantly higher than the 'critical micelle concentration' for the formation of SDS micelles in our buffers). The pKm value was 5.6. This value, although significantly higher than the value of ~2.8 for MPIX dissolved in buffer in the absence of any detergents, was nevertheless lower than the value of 6.5 for the MPIX–PS5.M complex. Although it would be rash to overinterpret the above data, it does appear that saturation binding to SDS micelles does not enhance the basicity of MPIX quite as well as its binding to the DNAzyme.

The above data, as well as the strikingly preferential binding of NMM by the DNAzyme (three orders of magnitude better than MPIX binding), allow us to formulate a hypothesis that the increase in basicity (and hence also the ease of metallation) observed for MPIX bound to the DNAzyme may be due to a distortion of the planar structure of MPIX by the enzyme. However, we cannot rule out at this stage the possibility that the catalytic effect of PS5.M. may arise in whole or in part from a strategic positioning of negatively charged phosphate group(s) that stabilize the incipient positive charge of the protonation (or metallation) transition state.

In summary, our insight into the *modus operandi* of this very small but catalytically efficient DNAzyme helps broaden our insight into the sophistication of sites within nucleic acids for the binding of small molecules and, by extension, of active sites within nucleic acid enzymes. From our results, it appears likely that a pronounced and measurable enhancement of substrate basicity by the DNAzyme is, in fact, the means by which it accomplishes its catalytic task.

The physical basis for this basicity increase is more difficult to be certain about at this stage, and will probably have to await high-resolution structural data on the enzyme–substrate complex. Efforts at crystallization of the MPIX–DNAzyme complex are currently underway.

Significance

Here we provide experimental evidence regarding the *modus operandi* of a small but efficient DNA enzyme (DNAzyme), PS5.M, that catalyzes the metallation of mesoporphyrin IX (MPIX) by copper and zinc ions. The MPIX–DNAzyme complex has an absorption spectrum resembling not so much those of the free porphyrin MPIX (in its solution-aggregated and its monomeric forms) but rather that of the DNAzyme complexed to a distorted porphyrin, *N*-methylmesoporphyrin (NMM). NMM is recognized as a stable transition state analog for the metallation reaction. pH titration experiments reveal that the DNAzyme enhances the basicity (and hence the ease of metallation) of the substrate, MPIX, by 3–4 pH units. The DNAzyme may cause this basicity enhancement by distortion of the planar porphinato– core of MPIX to resemble that of the naturally deformed porphyrin, NMM, or by stabilization by a DNA phosphate of the growing positive charge in the transition state for porphyrin protonation/metallation, or by a combination of the two. This catalytic strategy of enhancing substrate basicity may also hold true for the recently described catalytic RNA and catalytic antibody for porphyrin metallation. Our results serve to illuminate a strategy by which primordial nucleic acid enzymes in an RNA world might have catalytically generated this important class of enzymatic cofactors — the metalloporphyrins.

Materials and methods

Materials

DNA oligomers were synthesized at the University Core DNA Services (University of Calgary). Synthesized sequences for DNAzyme assays were purified as follows: the oligomers were first size-purified in denaturing polyacrylamide gels. The eluted DNA (in TE buffer: 10 mM Tris, pH 7.4; 0.1 mM EDTA) was then passed through Spice C18 (Rainin) columns. The bound DNA was released from these columns with 30% acetonitrile. Following lyophilization, the purified DNA oligomers were dissolved in 10 mM Tris acetate, pH 7.4, and stored at −20°C. All salt solutions were avoided during the above purification procedure because the presence of metal ions (including Mg^{2+}, Na^{+} and K^{+}) was found to affect the catalytic rates of the DNAzymes. For the experiments described in this paper, all DNA oligomers were first heat denatured in 10 mM Tris acetate buffer (see above) at 90°C, for 5 min, and then allowed to cool slowly to room temperature. The sequences of the various DNA oligomers studied are given below:

PS5.ST1 (33 nucleotides):

TCGTG GGTCA TTGTG GGTGG GTGTG GCTGG TCC

PS5.M (24 nucleotides):

GTGGG TCATT GTGGG TGGGT GTGG

PS19.ST1 (23 nucleotides):

AGGTT ATAGG GCGGG AGGGT GGT

PS2.M (18 nucleotides):

GTGGG TAGGG CGGGT TGG

TM.M2 (18 nucleotides):

GTGGG TTGGG TGGGT TGG

OXY4 (32 nucleotides):

TTTTG GGGTT TTGGG GTTTT GGGGT TTTTGG GG

BLD (27 nucleotides):

AATAC GACTC ACTAT AGGAA GAGAT GG

Porphyrins. The porphyrins (MPIX and NMM) were purchased from Porphyrin Products (Logan, Utah), and used without further purification. Their concentrations in aqueous solutions were determined using standard methods [43].

Spectroscopy

UV–visible absorption measurements on both MPIX and NMM were carried out in a dual-beam Cary 3E UV-Visible Spectrophotometer, at 20°C. Fluorescence measurements were carried out in a Photon Technology International (PTI) Spectrofluorimeter.

Titration of MPIX and NMM absorptions with nonionic detergents

MPIX solutions [2 μM diluted from a 100 μM stock solution in 40K+T buffer (100 mM MES, 50 mM Tris, 40 mM potassium acetate, 0.25% Triton X-100, 1% DMSO, final pH 6.2)] were individually made in 40K buffer (which contained all the components of 40K + T buffer except the Triton and the DMSO) containing different concentrations of either Triton X-100, Tween 20, or Nonidet P-40. These solutions were scanned over the wavelength range 300 to 700 nm. Various concentrations for each detergent were tested to determine the detergent concentration at which MPIX started to give saturated absorption profiles.

Porphyrin absorption in the presence of various DNA oligomers

The comparison of the effects of different DNA oligomers on the absorption spectra of MPIX was carried out using solutions containing 1 μM MPIX and 10 μM DNA, in 40K buffer, at 20°C. For UV–visible absorption spectra of MPIX titrated with increasing concentrations of PS5.M, the MPIX concentration was fixed at 1 μM while the PS5.M concentrations were at, variously, 0, 1, 3, 5, 7, 9, 12, 15, 20, 30, 50, 75, 100, 150, 200, 250, 300 and 366 μM. The solutions were prepared as follows: DNA was first incubated in 40K buffer for 20 min, to allow proper folding of the oligomer; then MPIX was introduced (from 100 μM stocks in 40K+T, containing 0.25% Triton X-100). The mixtures were incubated for 10 min before their spectra were recorded. For the titration by PS5.M of NMM UV–visible absorption, a fixed concentration of 1 μM NMM was used, and DNA concentrations were varied up to 20 μM.

Fluorescence measurements

The emission spectra of both NMM and MPIX were recorded with the excitation wavelength set at 397 nm. The emission spectral scan range was between 500 nm and 720 nm. The spectra were taken at room temperature (22°C).

Binding constant measurements

MPIX. Absorption experiments were carried out to obtain the binding constant of MPIX to PS5.M. A series of MPIX–PS5.M solutions, in 40K buffer, were prepared. All solutions contained 1 μM MPIX; but, contained PS5.M at concentrations of 0, 1, 3, 5, 7, 10, 15, 20, 25, 40, 50, 100 and 150 μM, respectively. These solutions were incubated for 20 min at room temperature and their absorption spectra were taken in the 350 to 650 nm range. The absorbance versus PS5.M concentration dependence obtained was fitted to the following equation described by Wang *et al.* [48]: $[DNA]_0 = K_d\,(A - A_0)/(A_\infty - A) + [P]_0\,(A - A_0)/(A_\infty - A_0)$, where $[DNA]_0$ and $[P]_0$ are the initial concentrations of PS5.M and MPIX, respectively. A, A_∞ and A_0 are, respectively, the absorbance readings of the MPIX–PS5.M sample at different DNAzyme concentrations; the fully-bound MPIX; and the totally free (DNAzyme–unbound) MPIX.

NMM. Fluorescence experiments were carried out to obtain the binding constant of NMM to PS5.M, in 40K buffer. The NMM concentration was fixed at 25 nM; to this solution were added pre-folded PS5.M (in 40K buffer), to give final DNAzyme concentrations of 2, 7, 13, 25, 35, 45, 55, 65, 75, 85, 95, 105, 125, 145, 165, 185 and 205 nM. Samples were excited at 397 nm, and emission spectra were recorded from 580 to 700 nm. The fluorescence intensities obtained were incorporated into the above equation to derive the K_d value.

pH titrations using absorbance

Buffer solutions with different pH values were made as follows (using standard procedures): pH 1.0–2.0 solutions were buffered with HCl-NaCl; pH 2.0–3.6 with glycine-HCl; pH 3.7–5.6 with sodium (or potassium) acetate-acetic acid; pH 5.8–8.0 with Na_2HPO_4-NaH_2PO_4 (or their potassium salts); pH 7.0–9.0 with Tris-HCl; pH 8.6–10.6 with glycine-NaOH (or KOH); pH 11.0–12.0 with Na_2HPO_4-NaOH; and pH 12.0–13.0 with NaOH-NaCl. All buffer solutions contained either 100 mM K^+ or 100 mM Na^+. Potassium ions had to be used for PS5.M (for the formation of the catalytically active folded structure of PS5.M see [32]), while sodium ions had to be used for solutions containing SDS (SDS precipitates in the presence of even low concentrations of potassium). While the porphyrin–Triton or the porphyrin–SDS solutions were tested for the entire pH range from 1.0 to 13.0, porphyrin–PS5.M solutions were tested only in the range of pH 4.0 to pH 10.0. For these experiments the NMM concentration was fixed at 3 μM; the MPIX concentration (where relevant) at 1 μM; PS5.M at 20 μM (to provide approximately 80% binding of 1 μM MPIX); and, where relevant, Triton X-100 at 0.1% (sufficient, again, to solubilize the 1 μM MPIX); and SDS at 1%.

pH titrations using fluorescence

Fluorescence titration experiments were carried out to derive the pKa value of MPIX in solution containing neither Triton nor DNAzyme, in a solution containing 0.1% Triton only, and in a solution containing 1μM PS5.M. In all of these, MPIX concentration was fixed at 10 nM. The excitation wavelength used was 397 nm.

Calculations

A porphyrin sample at a specific pH may contain proportions of both the neutral (P) and mono-protonated (PH^+) forms of the porphyrin. The ionization equilibrium, of course, is simply described by:

$$PH^+ \overset{K_a}{\rightleftharpoons} H^+ + P$$

Therefore, $K_a = [H^+][P]/[PH^+]$ and, $\log K_a = \log [H^+] + \log \{[P]/[PH^+]\}$. If the total porphyrin concentration equals c, $\{c = [PH^+] + [P]\}$, we can define [P] as x. Then, $[PH^+] = c - x$. Therefore, $[PH^+]/[P] = (c-x)/x = (c/x) - 1$.

Now, if A is the absorbance of a porphyrin sample (containing both protonated and unprotonated forms, PH^+ and P) at a given pH, and two quantities, A_1 and A_2, are defined such that they represent the saturating absorbances of the porphyrin sample at, respectively, the basic and acidic ends of the titration spectrum for that porphyrin, we can write the following relationship:

$$c/x = (A_2 - A_1)/(A - A_1)$$

Therefore:

$$\log k_a = \log [H^+] - \log [(A_2 - A_1)/(A - A_1) - 1]$$

Therefore:

$$\log [(A_2 - A_1)/(A - A_1) - 1] = -\log k_a + \log [H^+] = pK_a - pH \quad (1)$$

For the situation where the porphyrin can undergo two protonation events, we have the equlibria:

$$PH_2^{2+} \overset{K_{a1}}{\rightleftharpoons} H^+ + PH^+, \text{ and } PH^+ \overset{K_{a2}}{\rightleftharpoons} H^+ + P$$

In the case of porphyrins such as MPIX, where these two protonation events are essentially concurrent (two protonation events, but a single effective pK_a for protonation), $K_{a1} = K_{a2} = 'K_a'$. In this instance, Equation 1 (above) would be modified to give:

$$\log [(A_2 - A_1)/(A - A_1) - 1] = 2pK_a - 2pH \quad (2)$$

To generalize this notion, if there are multiple (n) concurrent protonation events (n protonation events, but a single effective pK_a), Equation 2 would take the following form:

$$\log [(A_2 - A_1)/(A - A_1) - 1] = n\,pK_a - n\,pH \quad (3)$$

In other words, a plot of $\log [(A_2 - A_1)/(A - A_1) - 1]$ versus pH should give a straight line with a slope equal to $-n$, and the intercept on the x axis at the pK_a value.

Essentially identical formalisms can be derived for data consisting of fluorescence (rather than absorbance) measurements.

Acknowledgements

This work was supported by the Natural Sciences and Engineering Research Council of Canada (NSERC) and by the British Columbia Health Research Foundation (BCHRF). We are grateful to our colleagues in the Sen laboratory and to others at Simon Fraser University for their help and advice. We are particularly grateful to Andrew Bennet for his valuable insights and also for the use of his UV–visible spectrophotometer.

References

1. Kruger, K., Grabowski, P.J., Zaug, A.J., Sands, J., Gottschling, D.E. & Cech, T.R. (1982). Self-splicing RNA: autoexcision and autocyclization of the ribosomal RNA intervening sequence of tetrahymena. *Cell* **31**, 147-157.
2. Guerrier-Takada, C., Gardiner, K., Marsh, T., Pace, N. & Altman, S. (1983). The RNA moiety of ribonuclease P is the catalytic subunit of the enzyme. *Cell* **35**, 849-857.
3. Cech, T.R. (1993). Structure and mechanism of the large catalytic RNAs: group I and group II introns and ribonuclease P. In *The RNA World.* (Gesteland, R. F. & Atkins, J.F., eds), pp. 239-269, Cold Spring Harbor Laboratory Press: Cold Spring Harbor, NY.
4. Long, D.L. & Uhlenbeck, O.C. (1993). Self-cleaving catalytic RNA. *FASEB J.* **7**, 25-30.
5. Noller, H.F., Hoffarth, V. & Zimniak, L. (1992). Unusual resistance of peptidyl transferase to protein extraction procedures. *Science* **256**, 1416-1419.
6. Lorsch, J.R. & Szostak, J. W. (1996). Chances and necessity in the selection of nucleic acid catalysts. *Acc. Chem. Res.* **29**, 103-110.
7. Breaker, R.R. (1997). *In vitro* selection of catalytic polynucleotides. *Chem. Rev.* **97**, 371-390.
8. Osborne, S.E. & Ellington, A. D. (1997). Nucleic acid selection and the challenge of combinatorial chemistry. *Chem. Rev.* **97**, 349-370
9. Gilbert, W. (1986). The RNA world. *Nature* **319**, 618.
10. Joyce, G.F. & Orgel, L.E. (1993). Origin of The RNA World. In *The RNA world.* (Gesteland, R.F. & Atkins, J.F., eds) pp. 1-25, Cold Spring Harbor Laboratory Press: Cold Spring Harbour, NY.
11. Breaker, R.R. & Joyce, G.F. (1994). A DNA enzyme that cleaves RNA. *Chem. Biol.* **1**, 223-229.
12. Cuenoud, B. & Szostak, J.W. (1995). A DNA metalloenzyme with ligase activity. *Nature* **375**, 611-614.
13. Breaker, R.R. & Joyce, G.F. (1995). A DNA enzyme with Mg^{2+}-dependent RNA phosphoesterase activity. *Chem. Biol.* **2**, 655-660.
14. Li, Y. & Sen, D. (1996). A catalytic DNA for porphyrin metallation. *Nat. Struct. Biol.* **3**, 743-747.
15. Carmi, N., Schultz, L.A. & Breaker, R.R. (1996). *In vitro* selection of self-cleaving DNAs. *Chem. Biol.* **3**, 1039-1046.
16. Santoro, S.W. & Joyce, G.F. (1997). A general-purpose RNA-cleaving DNA enzyme. *Proc. Natl Acad. Sci. USA.* **94**, 4262-4266.
17. Geyer, C.R. & Sen, D. (1997). Evidence for the metal cofactor-independence of a RNA phosphodiester cleaving DNAzyme. *Chem. Biol.* **4**, 579-593.
18. Lavallee, D.K. (1988). Porphyrin metalation reactions in biochemistry. *Mol. Struct. Energ.* **9**, 279-314.
19. Cochran, A.G. & Schultz, P.G. (1990). Antibody-catalysed porphyrin metallation. *Science* **249**, 781-783.

20. De Matteis, F., Gibbs, A.H. & Tephly, T.R. (1980). Inhibition of protohaem ferro-lyase in experimental porphyria. *Biochem. J.* **188**, 145-152.
21. Tephly, T.R., Gibbs, A.H., & De Matteis, F. (1979). Studies on the mechanism of experimental porphyria produced by 3,5-diethoxycarbonyl-1,4-dihydrocollidine. *Biochem. J.* **180**, 241-244.
22. Ortiz de Montellano, P.R., Berlan, H.S. & Kunze, K.L. (1981). *N*-methyl-protoporphyrin IX: chemical synthesis and identification as the green pigment produced by 3,5-diethoxycarbonyl-1,4-dihydrocollidine treatment. *Proc. Natl Acad Sci. USA* **78**, 1490-1494.
23. Dailey, A.D. & Fleming, J.E. (1983). Bovine ferrochelatase. *J. Biol. Chem.* **258**, 11453-11459.
24. Goldberg, D.E. & Thomas, K.M. (1976). Crystal and molecular structure of an *N*-substituted porphyrin, chloro (2,3,7,8,12,13,17,18-octaethyl-*N*-ethylacetatoporphine) cobalt (II). *J. Am. Chem. Soc.* **98**, 913-919.
25. Lavallee, D.K. (1982). Crystal and molecular structure of a free-base *N*-methylporphyrin: *N*-methyl-5,10,15,20-tetrakis(p-bromophenyl)porphyrin. *J. Am. Chem. Soc.* **104**, 4707-4708.
26. McLaughlin, G. (1974). Crystal and molecular structure of a non-metallo, *N*-substituted porphyrin, 21-ethoxycarbonylmethyl-2,3,7,8,12,13,17,18-octaethylporphyrin. *J. Chem. Soc. Perkin Trans.* **2**, 136-140.
27. Bain-Ackerman, M.J. & Lavallee, D.K. (1979). Kinetics of metal-ion complexation with *N*-methyltetraphenylporphyrin. Evidence concerning a general mechanism of porphyrin metallation. *Inorg. Chem.* **18**, 3358-3364.
28. Matsushima, Y. & Sugata, S. (1979). Kinetics of incorporation of manganese(II), cobalt(II), and nickel(II) into tetraphenylporphine in dimethylformamide. Effects of the acetate anion. *Chem. Pharm. Bull.* **27**, 3049-3053.
29. Shah, B., Shears, B. & Hambright, P. (1971). Kinetic differences between the incorporation of zinc(II) and cadmium(II) into porphyrins and n-methylporphyrins. *Inorg. Chem.* **10**, 1828-1830.
30. Schultz, P.G. & Lerner, R.A. (1995). From molecular diversity to catalysis: lessons from the immune system. *Science* **269**, 1835-1842.
31. Conn, M.M., Prudent, J.R. & Schultz, P.G. (1996). Porphyrin metallation catalyzed by a small RNA molecule. *J. Am. Chem. Soc.* **118**, 7012-7013.
32. Li, Y. & Sen, D. (1997). Toward an efficient DNAzyme. *Biochemistry.* **36**, 5589-5599.
33. Sen, D. & Gilbert, W. (1992). Guanine quartet structures. *Methods. Enzymol.* **211**, 191-199.
34. Williamson, J.R. (1994) G-quartet structures in telomeric DNA. *Annu. Rev. Biophys. Biomol. Struct.* **23**, 703-730.
35. Li, Y., Geyer, C.R. & Sen, D. (1996). Recognition of anionic porphyrins by DNA aptamers. *Biochemistry* **35**, 6911-6922.
36. Brown, S.B. & Shillcock, M. (1976). Equilibrium and kinetic studies of the aggregation of porphyrins in aqueous solution. *Biochem. J.* **153**, 279-285.
37. Brown, S.B. & Hatzikonstantinou, H. (1978). The dimerization of ferrihaems. *Biochim. Biophys. Acta.* **539**, 338-363.
38. Brown, S.B. Hatzikonstatinou, H., & Herries, D. (1980). The structure of porphyrins and haems in aqueous solution. *Int. J. Biochem.* **12**, 701-707.
39. Karns, G.A., Gallagher, W.A. & Elloit, W.B. (1979). Dimerization constants of water-soluble porphyrins in aqueous alkali. *Bioorg. Chem.* **8**, 69-81.
40. Margalit, R. & Rotenberg, M. (1984). Thermodynamics of porphyrin dimerization in aqueous solutions. *Biochem. J.* **219**, 445-450.
41. Mazumdar, S. & Mitra, S. (1990). Aggregation in five-coordinate high-spin natural hemins: determination of solution structure by ^{1}H NMR. *J. Phys. Chem.* **94**, 561-566.
42. Falk, J.E. (1964). *Porphyrins and Metalloporphyrins.* Elsevier, New York.
43. Smith, K.M. (1964). In *Porphyrins and Metalloporphyrins* pp 11-12. Elsevier, Amsterdam.
44. Porra, R.J. & Jones, O.T.G. (1963). Studies on ferrochelatase. *Biochem. J.* **87**, 181-185.
45. Li, F., Lim, C.K. & Peters, T.J. (1987). An HPLC assay for rat liver ferrochelatase. *Biomedical Chromatography* **2**, 164-168.
46. Lavallee, D.K. (1987) *The Chemistry and Biochemistry of N-Substituted Porphyrins.* VCH, New York.
47. van Holde, K.E. (1985). *Physical Biochemistry*, 2nd edn. Prentice-Hall, Englewood Cliffs, NJ.
48. Wang, Y., Hamasaki, K. & Rando, R.R. (1997). Specificity of aminoglycoside binding to RNA constructs derived from the 16S rRNA decoding region and the HIV-RRE activator region. *Biochemistry* **36**, 768-779.
49. Dempsey, B., Lowe, M.B. & Phillips, J.N. (1961). The physico-chemical behaviour of porphyrins solubilized in aqueous detergent solutions. In *Haematin Enzymes* (Falk., J. E.,Lemberg, R. & Morton, R. K., eds) pp. 29-40, Pergamon, London.
50. Corwin, A.H., Chivvis, A.B., Poor, R.W., Whitten, D.G. & Baker, E.W. (1968). The interpretation of porphyrin and metalloporphyrin spectra. *J. Am. Chem. Soc.* **90**, 6577-6583.
51. Gouterman, M. (1978). Optical spectra and electronic structure of porphyrins and related rings. In *The Porphyrins*, Vol. III (Dolphin, D., ed.) pp. 1-163, Academic Press, New York.
52. Ogoshi, H., Watanabe, E. & Yoshida, Z. (1973). Porphyrin acids. *Tetrahedron* **29**, 3241-3245.
53. Stone, A. & Fleischer, E.B. (1968). The molecular and crystal structure of porphyrin diacids. *J. Am. Chem. Soc.* **90**, 2735-2748.
54. Hirayama, N., Takenaka, A. & Sasada, Y. (1974). X-ray crystal structure of octaethylporphinium (monocation) tri-iodide. *J. Chem. Soc. Chem. Comm.* 330-331.

Because *Chemistry & Biology* operates a 'Continuous Publication System' for Research Papers, this paper has been published via the internet before being printed. The paper can be accessed from http://biomednet.com/cbiology/cmb – for further information, see the explanation on the contents pages.